Inward Current in Single Smooth Muscle Cells of the Guinea Pig Taenia Coli

Y. YAMAMOTO, S. L. HU, and C. Y. KAO

From the Department of Pharmacology, State University of New York Downstate Medical Center, Brooklyn, New York 11203

ABSTRACT Using the tight-seal voltage-clamp method, the ionic currents in the enzymatically dispersed single smooth muscle cells of the guinea pig taenia coli have been studied. In a physiological medium containing 3 mM Ca^{2+}, the cells are gently tapering spindles, averaging 201 (length) × 8 μm (largest diameter in center of cell), with a volume of 5 pl. The average cell capacitance is 50 pF, and the specific membrane capacitance 1.15 $\mu F/cm^2$. The input impedance of the resting cell is 1–2 GΩ. Spatially uniform voltage-control prevails after the first 400 μs. There is much overlap of the inward and outward currents, but the inward current can be isolated by applying Cs^+ internally to block all potassium currents. The inward current is carried by Ca^{2+}. Activation begins at ~−30 mV, maximum I_{Ca} occurs at +10–+20 mV, and the reversal potential is ~+75 mV. The Ca^{2+} channel is permeable to Sr^{2+} and Ba^{2+}, and to Cs^+ moving outwards, but not to Na^+ moving inwards. Activation and deactivation are very rapid at ~33°C, with time-constants of <1 ms. Inactivation has a complex time course, resolvable into three exponential components, with average time constants (at 0 mV) of 7, 45, and 400 ms, which are affected differently by voltage. Steady-state inactivation is half-maximal at −30 mV for all components combined, but −36 mV for the fast component and −26 and −23 mV for the other two components. The presence of multiple forms of Ca^{2+} channel is inferred from the inactivation characteristics, not from activation properties. Recovery of the fast channel occurs with a time-constant of 72 ms (at +10 mV). Ca^{2+} influx during an action potential can transfer ~9 pC of charge, which could elevate intracellular Ca^{2+} concentration adequately for various physiological functions.

INTRODUCTION

Voltage-clamp studies on multicellular preparations have always been hampered by daunting technical difficulties, whether they were conducted on cardiac tissues or smooth muscle preparations. At a time when no alternative methods were available for dealing with the small individual cells in these tissues, those studies provided useful interim information, extending our knowledge beyond descriptive accounts based on monitoring resting and action potentials.

Address reprint requests to Dr. C. Y. Kao, Department of Pharmacology, SUNY Downstate Medical Center, 450 Clarkson Avenue, Brooklyn, NY 11203-9967. Dr. Yamamoto's permanent address is Department of Physiology, Nagoya City University Medical School, Nagoya, Japan.

J. GEN. PHYSIOL. © The Rockefeller University Press · 0022-1295/89/03/0521/30 $2.00
Volume 93 March 1989 521–550

The need for unambiguous data on the properties of ionic channels of smooth muscles was first satisfied when freshly dispersed single cells from amphibian stomachs were successfully impaled with conventional microelectrodes (Caffrey et al., 1980; Singer and Walsh, 1980; Walsh and Singer, 1981). Mammalian smooth muscle cells are generally smaller than those of amphibian origin, and their ionic channels were not properly studied until the development of successful regimens of enzymatic dispersion (Momose and Gomi, 1980; Obara, 1984) and the advent of the tight-seal patch-clamp technique (see Hamill et al., 1981).

A number of publications have now appeared describing various ionic channels in several types of mammalian smooth muscles, using the tight-seal technique (Benham and Bolton, 1983; Benham et al., 1985; Klöckner and Isenberg, 1985*a*, *b*; Mitra and Morad, 1985; Yoshino and Yabu, 1985; Bean et al., 1986; Caffrey et al., 1986; Droogmans and Callewaert, 1986; Ganitkevitch et al., 1986, 1987; Inoue et al., 1986; Ohya et al., 1986; Sturek and Hermsmeyer, 1986; Clapp et al., 1987). Many of these dealt primarily with single-channel events without showing the concomitant whole-cell basis or associations of such events. Although the single-channel data possess intrinsic interest, it would be desirable to have whole-cell information as a logical bridge between familiar physiological phenomena and their molecular basis. It is also desirable to have information on freshly dispersed cells in addition to that on cultured cells, which might be somewhat different.

We report here our studies on the freshly dispersed single myocytes from the guinea pig taenia coli, a preparation on which a wealth of information has already been accumulated (see Bülbring et al., 1981). This paper deals with some basic elements of ionic currents in the whole cell, and some details of the early transient inward current. Another paper deals with the outward current (Yamamoto et al., 1989), and a third paper deals with some single-channel events that we have been able to relate to the macroscopic currents in whole cells (Hu, S. L., Y. Yamamoto, and C. Y. Kao, manuscript submitted for publication). Preliminary results of these studies have been published (Hu et al., 1987*a*, *b*; Yamamoto et al., 1987*a*, *b*).

MATERIAL AND METHODS

Tissue and Cell Isolation

Male guinea pigs of 400–600 g were used. Single cells from the taenia coli were dispersed, using a modification of the method of Obara (1984). Isolated strips of taenia coli were incubated in a modified Krebs' solution, containing low calcium (0.18 mM) at 37°C for 30 min, and then transferred to a modified Krebs' solution containing no added calcium salts (solution A, Table I) for 15 min. Each strip, now relaxed, was then cut into pieces 1.5–2 cm long, which were incubated in an enzyme-dispersing medium, consisting of 0.2% (wt/vol) collagenase (350 U/mg type I, C-0130; Sigma Chemical Co., St. Louis, MO), 0.4% soybean trypsin inhibitor (type II-S, Sigma T-9128), and 0.6% bovine serum albumin.

After incubation at 37°C for 30 min with gentle stirring, the dispersing medium was replaced by solution A containing 1% bovine serum albumin in four separate washes. After the last wash, the tissue pieces were resuspended in solution A and incubated for 15 min at 37°C with stirring. Then they were rinsed and suspended in a modified "KB" solution, and triturated with a glass Pasteur pipette with a tip opening of ~2 mm. The modified "KB" solution (Isenberg and Klöckner, 1982), consisted of (in millimolar): 85 KCl, 30 K_2HPO_4, 5

TABLE I

Composition of Bath Solutions

	A	B	C	D	E	F	G
				mM			
NaCl	135.0	135.0	135.0	94.5	105.0	105.0	64.5
KCl	5.4	5.4	5.4	5.4	5.4	5.4	5.4
$MgCl_2$	1.0	1.0	1.0	1.0	1.0	1.0	1.0
$CaCl_2$	0	1.0	3.0	30.0	0	3.0	30.0
TEACl*	0	0	0	0	30.0	30.0	30.0
HEPES‡	10.0	10.0	10.0	10.0	10.0	10.0	10.0
Glucose	5	5	5	5	5	5	5

*Tetraethylammonium chloride.

‡*N*-2-hydroxyethylpiperazine-*N'*-2-ethanesulfonic acid. pH of all solutions was adjusted to 7.2–7.3 by the use of NaOH.

$MgSO_4$, 5 Na_2ATP, 5 K-pyruvate, 5 creatine, 20 taurine, 5 beta-hydroxybutyrate, 1 g/liter fatty-acid-free bovine albumin. The supernatant was checked for the presence of dispersed cells and discarded. The tissue material was resuspended in fresh "KB" solution and again triturated. Trituration was repeated until the supernatant contained about 100 cells per field at 100-fold magnification. Then the entire material was filtered on an 80-μm nylon mesh to remove undispersed tissue fragments. The filtrate generally contained cells suitable for these studies, and was stored in a refrigerator (6–8°C). Cells for the study were drawn from this stock, and removed into the experimental chamber (see below). Cells suitable for our work have been stored this way for up to 6 h.

Electrophysiological Techniques

The tight-seal method (see Hamill et al., 1981) was used. Electrodes were made from Kimax-51 capillary tubing of borosilicate glass (1.45-mm o.d.) and heat-polished on a microforge to finished tip openings of 1–2-μm diameter. The resistance of the electrodes when filled with "intracellular" solution (standard pipette solution, Table II) was ~2 MΩ. Other electrode solutions are given in Table II. For the present series of investigations, the electrodes were not coated with silicone rubber.

The experimental chamber consists of a plastic 30-mm culture dish, with a central volume reduced to 0.3 ml, and a glass coverslip at the bottom to which the dispersed cells generally adhered after a 20-min settling time. Prewarmed (32–34°C) experimental solutions (listed in

TABLE II

Composition of Pipette Solutions

	K	Cs
	mM	
KCl	140.0	0
CsCl	0	140.0
EGTA*	1.0	1.0
K_2ATP‡	2.0	2.0
HEPES§	10.0	10.0

*Ethylene glycol-bis(-amino ethyl ether) *N,N'* tetraacetic acid.

‡Potassium salt of adenosine triphosphate.

§pH adjusted to 7.2–7.3 by the use of KOH.

Table I), were perfused, individually, into the chamber continuously at a rate of ~1.5 ml/min. All experiments were performed at 400× magnification on an inverted microscope.

A List EPC-7 amplifier was used. Gigaohm seals (usually 5–10 GΩ) were established by the usual suction method (Hamill et al., 1981). Pulsatile suction was used to break the membrane in the micropipette. In our experience, the most consistently reliable method of applying the sharp pulsatile suction is to use a solenoid-actuated vacuum of ~500 mm Hg (source vacuum) in trains of pulses of 25-ms duration at ~20 Hz (Picospritzer; General Valve Corp., Fairfield, NJ). Membrane rupture, recognizable by a sudden increase in the capacitive artifact, usually occurred with the first vacuum pulse. Repeated pulses are necessary to reduce series resistance, possibly by enlarging the rupture or by preventing healing. Pulses of shorter duration often failed to rupture the membrane, whereas pulses much longer than 25 ms tended to damage the electrode-to-cell seal. The actual vacuum at the tip of the electrode is not known because of the uncertain attenuation caused by various elastic tubing used to connect the source to the electrode and the response time of the entire system to a relatively short step pressure change.

The capacitive artifacts were appropriately compensated, using the 10-turn potentiometers provided in the amplifier. As shall be shown later in the Results, the dial reading is an accurate measure of the total capacitance of the cell, as is that for the series resistance. About 60–70% of the series resistance is always compensated for, no attempt being made at more compensation to avoid oscillations and damage to the cell. Details of the different voltage protocols used will follow in the appropriate section in the Results. The current signal was filtered with a 3-pole low-pass filter furnished in the amplifier (cut-off frequency, 3 kHz).

By use of p-CLAMP software (Axon Instruments, Inc., Burlingame, CA) and associated analog-to-digital converter (32 μs per point) and interface, the signals were digitilized (12-bit resolution) and stored directly in an IBM PC/XT microcomputer. No further signal filtering was used. Correction of leakage current was made by digital subtraction of currents produced either by full negative pulses or by scaled negative and positive pulses. In all whole-cell current records shown in this and the following papers, all currents are measured from the level of the holding current. In most cases, because the holding potential was close to the resting potential, the holding current was minimal. Some analyses and plotting were performed with help of the Lotus 1-2-3 software (Lotus Development Corp., Cambridge, MA).

RESULTS

General Descriptions

Cell morphology. In cold "KB" solution most cells are long and fully relaxed. Once cells are bathed in 3 mM Ca^{2+} solution at 33°C, they tend to contract either immediately or gradually. They also contract in response to applications of acetylcholine. In the present experiments, contracted cells were not used. Although noncontracted cells can survive for several hours, cells that have been exposed to Ca^{2+} for more than 1 h are routinely not used.

Morphometric parameters important for understanding physiological functions were measured from representative cells such as those shown in Fig. 1. The pertinent dimensions are as follows: For cells in the "KB" solution, the cell length is 262.9 ± 9.6 μm (means ± SEM of 19 cells). The widest diameter, where the nucleus usually resides, is 7.9 ± 0.3 μm; whereas the average diameter over the entire tapered cell is 5.3 ± 0.1 μm. The plate area is 1,387.6 ± 67.3 μm^2, and the surface area is 4,359.3 ± 211.4 μm^2 ($\pi \times$ plate area). The cell volume is 6.3 ± 0.4 pl. In

solutions containing 3 mM Ca^{2+}, the cells are shorter (average length, 200.8 ± 7.6 μm, $n = 14$) and fatter (average maximum diameter, 8.3 ± 0.4 μm). The surface area is 3,387.7 ± 166.5 μm^2, and the cell volume is 5.1 ± 0.4 pl.

Resting and action potentials and total membrane currents. The resting and action potentials of the dispersed cells were not systematically recorded, but in a smaller series of observations, the resting potential averaged −41.3 ± 0.63 mV ($n = 18$) in 1 mM Ca^{2+}. The peak of the action potential averaged +18.2 ± 1.1 mV ($n = 21$) in 1 mM Ca^{2+}, and +28.3 ± 0.9 mV ($n = 7$) in 3 mM Ca^{2+}. As the input impedance of the resting cell was ~1–2 GΩ (see below), and the seal resistance was usually 5–10 GΩ, the resting potential could have been shunted by 10–20%. However, the action potential, generated when the membrane conductance is considerably higher, would not have been significantly reduced. Cells for the main study were selected on the basis of an absence of spontaneous contractions and for their low leakage conductance. In most cells, spontaneous action potentials were induced upon release from the voltage clamp.

Fig. 2 shows the characteristic responses of a good quality cell in 1 mM Ca^{2+}. Under current clamp, a membrane time constant of 77.5 ms was found in the inward-current hyperpolarizing responses. On outward-current depolarization, spikes with peak amplitudes of 54–62 mV were recorded (Fig. 2 *A*). Because the current pulse was maintained for 250 ms, repetitive discharges were elicited. In the voltage-clamp mode (Fig. 2 *B*), depolarizing steps led to the familiar waveforms of an initial inward current followed by a more sustained outward current. It is clear that there is a considerable degree of temporal overlap between these currents (see below). For detailed analysis of the individual currents, we will rely on various procedures that are effective in isolating either the inward or the outward current.

Fig. 3 shows the influence of external $[Ca^{2+}]$ on the action potential and the underlying membrane current. For a cell in 1 mM Ca^{2+} (Fig. 3 *A*), the maximum diastolic potential was −45 mV, and the spike peaked at +14 mV. The fast depolarizing phase rose at a rate of 4.1 V/s. Since the total cell capacitance was 42.2 pF, the capacitive current ($C * dV/dt$) amounts to 173 pA. For a cell in 3 mM Ca^{2+} (Fig. 3 *B*, total capacitance 49.1 pF), the resting potential was −43.5 mV and the spike peaked at +31.7 mV. The fast depolarizing phase rose at 10.1 V/s, giving a capacitive current of 496 pA. This value is equivalent to 11.4 $\mu A/cm^2$, which is somewhat less than the maximum I_{Ca} in 3 mM Ca^{2+} under voltage-clamp conditions (see below), no doubt because of some overlap of I_K.

Membrane constants and series resistance. As estimated from small hyperpolarizations (current clamp), the input impedance of the quiescent resting cell averaged 1–2 GΩ. Such a high input impedance has also been observed in single toad stomach smooth muscle cells (Singer and Walsh, 1980; Walsh and Singer, 1987), and may be a common feature of smooth muscle cells.

The total cell capacitance, determined from the amount of compensation needed to cancel the capacitive artifact, averaged 50.14 ± 0.52 pF ($n = 209$). The validity of this procedure had first been established in a few cells in which the capacitive current was recorded at a fast time base, and the charge displaced was determined by integration (Fig. 4). The capacitance values found by the two methods agreed to 1%.

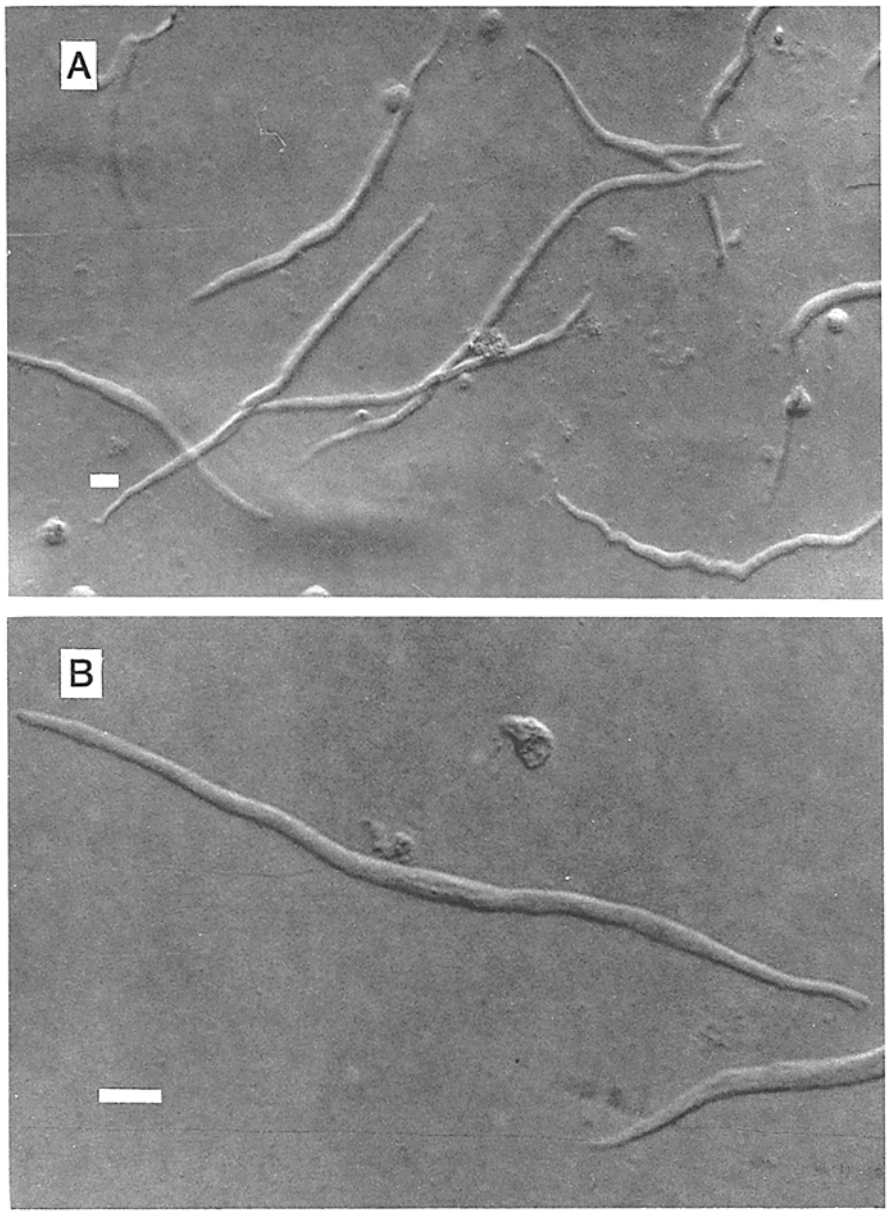

FIGURE 1. Dispersed cells of guinea pig taenia coli in "KB" medium. See text for details of dispersion technique. Scale bar, 20 μm in all frames. (*A*) At low magnification, most cells are relaxed, with an appearance suitable for present studies. (*B* and *C*) Two long and relaxed cells. The other cell in each frame is damaged and unsuitable. (*D*) Three cells showing different degrees of contraction. Only the bottom cell would be considered suitable for the present studies. Morphometric measurements were made from enlarged photographs of 19 relaxed cells, using a digitalizing pad (DT114; Houston Instruments, Austin, TX). Each cell was divided into 15–30 segments, with their ends perpendicular to the long axis of cell; each segment was treated as a short cylinder.

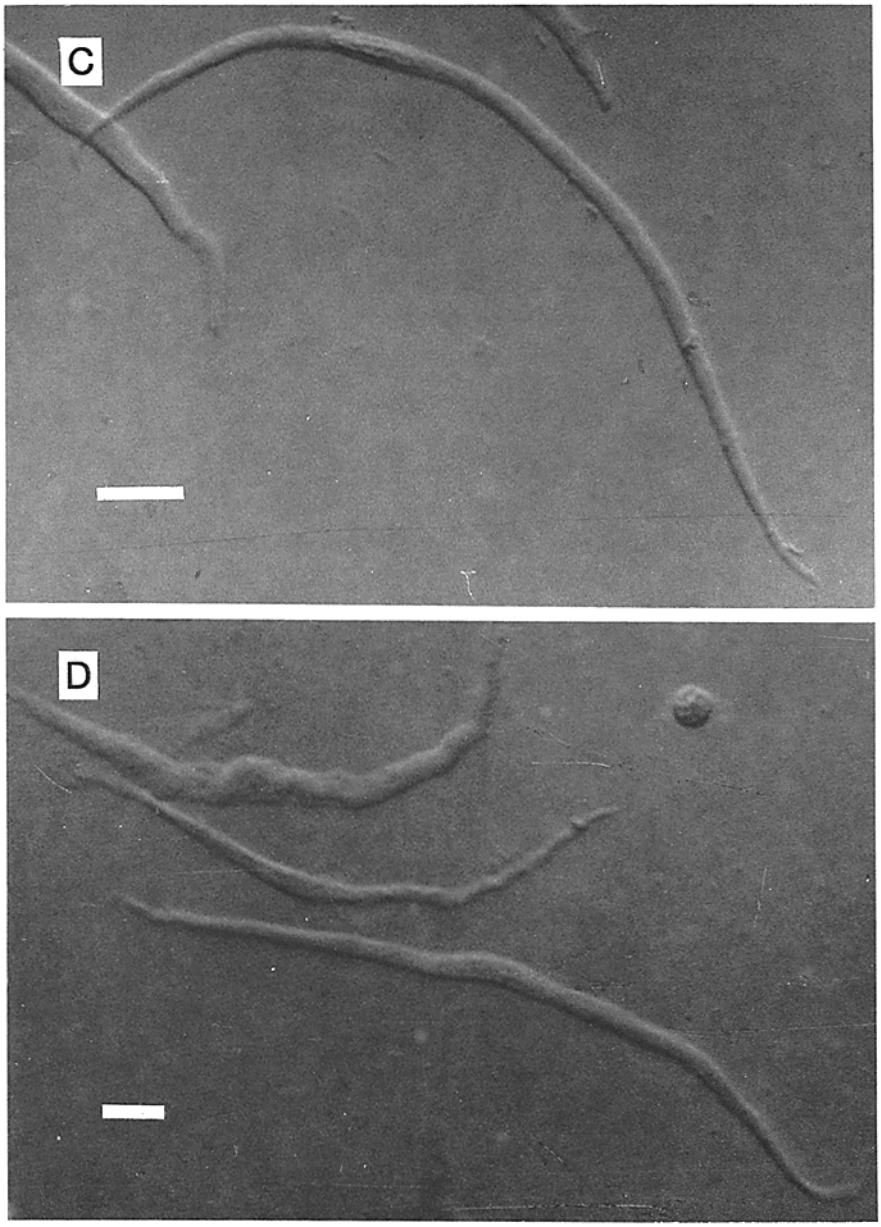

FIGURE 1. *(Continued)*

Assuming a specific membrane capacitance of 1 $\mu F/cm^2$, the membrane area of an average cell can be estimated to be 5,000 μm^2. This value is in unexpectedly good agreement with that derived from morphometric estimates. Alternatively, the specific membrane capacitance can be estimated from the average cell capacitance and average surface area (50.14 pF/4,359.3 μm^2), as 1.15 $\mu F/cm^2$.

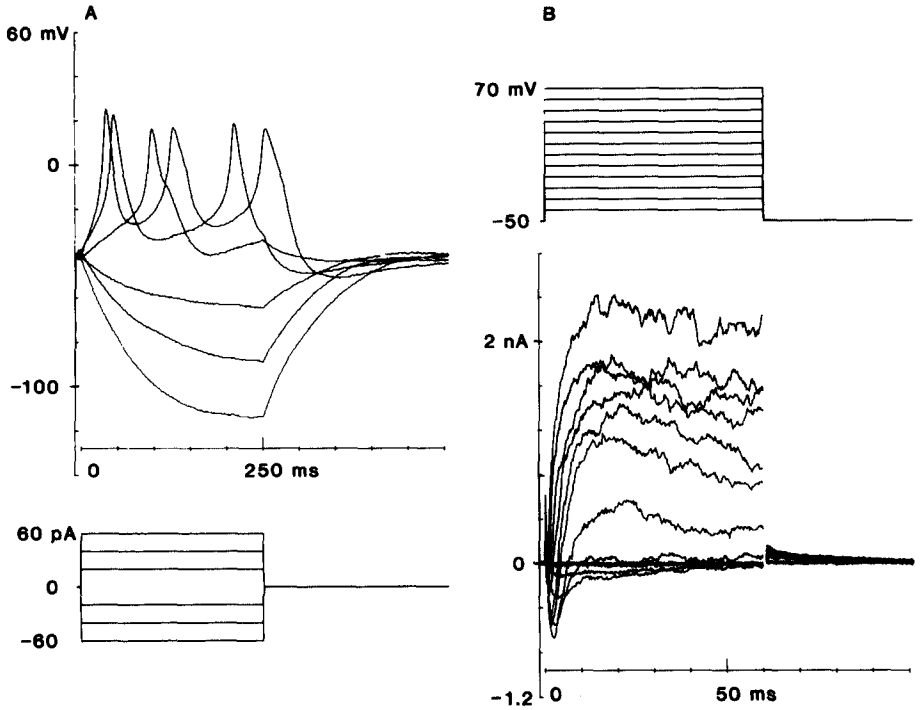

FIGURE 2. Whole-cell responses under current-clamp and voltage-clamp conditions. $[Ca^{2+}]_o$ is 1 mM (solution B, Table I). Temperature, 34°C. Resting potential, −40 mV. Total cell capacitance, 46.3 pF. (*A*) Current clamp. Applied current, three steps each in inward (downward traces, negative polarity) and outward (upward traces, positive polarity) directions are shown in the bottom trace. Membrane responses to applied current are shown in the top trace. On inward current-hyperpolarization, the membrane time constant is 77.5 ms. On outward current-depolarization, a single action potential was elicited with lowest current, and two and then three action potentials were elicited with higher currents. The shortest interval between repetitive spikes is ~100 ms (see Discussion). (*B*) Voltage clamp. Voltage steps are shown in the top trace; holding potential −50 mV; depolarizing steps were of 60 ms in duration in 10-mV increments up to +70 mV. Net membrane currents are in the bottom trace. These have been corrected for leakage, using hyperpolarizing steps. Capacitance compensation was applied, and residual uncorrectable capacitive artifact is visible as a sharp positive current spike at the beginning of the trace. For clarity, capacitive artifact at the break of voltage step has been omitted from the figure. Note the usual transient inward (negative) current followed by more gradual outward (positive) current, and the considerable overlap of two currents. Still, maximum inward current was reached at ~2 ms. The small outward tail current indicates that the holding potential of −50 mV is positive to potassium equilibrium potential of this cell.

The series resistance estimated from the amplifier control was ~2 MΩ. In a few cells, the series resistance was also estimated from the capacitive current as illustrated in Fig. 4. As the current due to a 9.8-mV step surged to 4.6 nA, the series resistance could be 2.13 MΩ. Because the initial surge could also be attenuated by small stray capacitance, the series resistance was also estimated from the time constant of decay of the capacitive current (Fig. 4). For the cell illustrated in Fig. 4, the

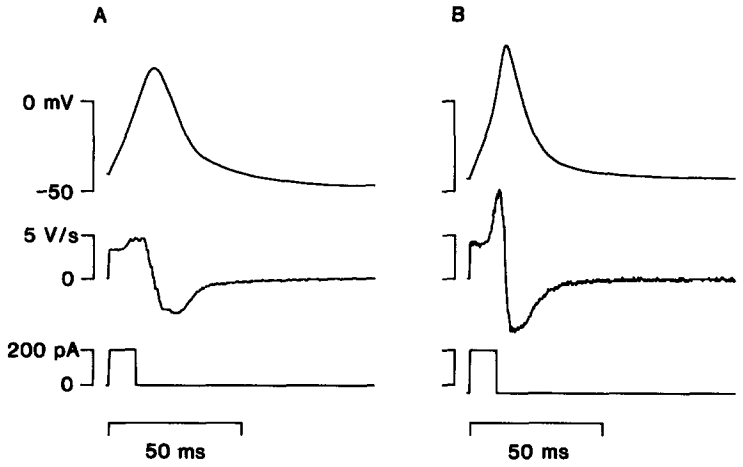

FIGURE 3. Action potentials elicited by brief current pulses in two cells in different $[Ca^{2+}]_o$. Top trace, membrane potential; middle trace, differentiated trace of voltage, dV/dt; bottom trace, applied current. (*A*) 1 mM Ca^{2+} (solution B, Table I); cell capacitance, 42.2 pF; maximum dV/dt, 4.1 V/s; temperature, 33°C. (*B*) 3 mM Ca^{2+} (solution C); cell capacitance, 49.1 pF; maximum dV/dt, 10.1 V/s; temperature, 33°C. Also see text for other details.

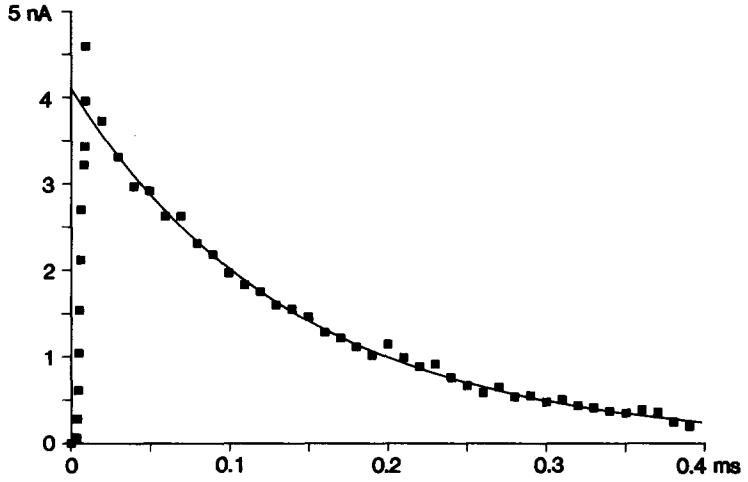

FIGURE 4. Capacitive current produced by 9.8-mV depolarization from holding potential of −50 mV. For this work, a digital oscilloscope (model 2090; Nicolet Instrument Corp., Madison, WI) was used, sampling at 0.5 μs per point. For clarity, only every 20th point of actual record in decay phase is plotted in the figure (square symbols). An artifact due to stray capacitance has been subtracted using current recorded before rupturing the cell. Amplifier band width, 100 kHz. Capacitive current surged to 4.6 nA. Except for the initial 10 μs, decay is well fitted with single exponential ($I = 4.1 \exp[-t/0.141]$). Integration of the area under the curve leads to a cell capacitance of 59.0 pF, compared with the amplifier reading of 59.5 pF. Series resistance calculated from the initial surge is 2.13 MΩ; from the time constant of current decay it is 2.37 M. The latter value is identical to equivalent amplifier reading. $[Ca^{2+}]_o$ = 3 mM (solution C).

series resistance so determined is 2.37 MΩ. In four other cells, the series resistance determined from the decay of the capacitive current was in very good agreement with the equivalent value on the amplifier control, justifying our reliance on the amplifier control reading.

The series resistance tended to increase during the experiment, and required frequent checking. Routinely, 60–70% of the series resistance was compensated for, leaving an effective series resistance of ~1 MΩ. For purposes of comparison with other studies on other cells (e.g., Klöckner and Isenberg, 1985*a*), the effective series resistance would be somewhat < 40 Ω-cm^2, or about an order of magnitude lower than that encountered in multicellular preparations (Kao and McCullough, 1975). For membrane currents of nanoamperes, no significant voltage error is incurred, but for currents of tens of nanoamperes, such as might flow through the potassium channel during large depolarizations, a significant error could exist.

Spatial voltage distribution. Because of the slender elongated shape of the individual taenia coli cell, there is a question whether spatially uniform voltage clamp can be attained by the tight-seal patch-clamp technique with the electrode tip applied only to a small central area of the cell. Fig. 5 shows the observations obtained from an experiment to assess the voltage distribution in the elongated cells used in the present study. Two separate tight-patch electrodes were used in the whole-cell mode with two separate amplifiers. One electrode (electrode 1) was placed at the midportion, and used for voltage-clamp commands and current recording. A second electrode (electrode 2) was placed 35 μm away towards one end, and was used for voltage monitoring. After correcting for a small difference in the DC-offset in the amplifiers (details in legend of Fig. 5), responses to a step to +10 mV at the two sites agreed to within 0.1 mV. In the same cell, after a number of other tests had been performed, and when some increase in series resistance was expected, a repeat check was made at command voltages to −10 and +10 mV. The voltage recorded at each site is within 1.5 mV of the command and of the other. So, the central 70 μm of the cell is isopotential, and the spatial decay for the remaining ends of the cell, calculated from open-end short cables, is negligible. It is significant that at +10 mV, the initial inward current is usually at its maximum (e.g., Fig. 6), and the space constant of the cell is close to its shortest. Also, −10 mV is in the negative resistance region where voltage control is most difficult. Therefore, these observations provide a basis for confidence in the adequacy of the steady-state spatial voltage control in these experiments.

Another relevant feature of voltage control is also evident in the records of Fig. 5. At V2, the command step was fully attained within 400 μs of the start of the voltage step. As the peak of the maximum inward current was reached at 2.1 ms, most of the ionic current phenomena to be detailed in the following were clearly obtained from cells that were spatially isopotential. The one aspect requiring particular caution concerns the kinetics of activation and deactivation of the early inward current, because incomplete capacitive compensation could easily delay the attainment of the command voltage.

Inward Current

As shown in Fig. 2, in the taenia myocytes at 32–34°C, there is considerable overlap of the inward and outward currents. To study the inward current in detail, the out-

ward current is blocked by using a pipette solution containing 140 mM Cs^+ (Table II), and an extracellular bath solution contained 30 mM tetraethylammonium (TEA; see Klöckner and Isenberg, 1985*a*, *b*).

The amplitude of the inward current did not remain constant indefinitely, but tended to decline with time (so-called "run-down"). The rate of "run-down" varied from cell to cell, no doubt depending on the quality of the dispersed cell. Generally, the observations described in this paper are based on cells in which little run-down was noted in ~40 min. More importantly, where a test condition was to be compared with a control condition, the control was always taken immediately before the test was applied. Observations made on any cell that did not maintain the same inward current amplitude within the first 15 min were discarded.

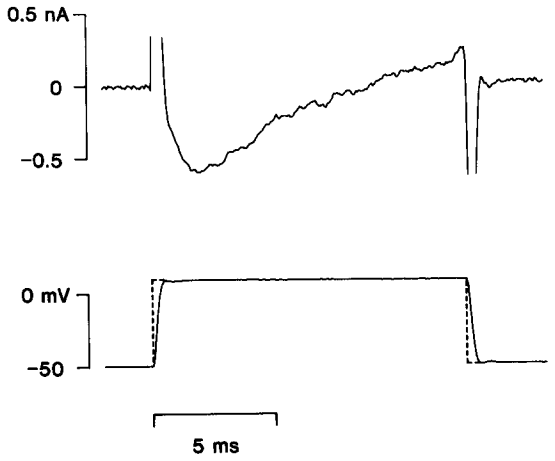

FIGURE 5. Test of spatial uniformity of single taenia coli myocyte under tight-seal voltage clamp. See text for other details. Cell was 175 μm long. Top trace is from electrode 1, placed in the middle of the cell, which measured 7.3 μm diameter. After rupture of the membrane, the electrode was used for voltage-clamping and current recording. The depolarizing step was 12.8 ms in duration to +10 mV. The bottom trace is voltage recorded with another electrode (2), at a point 35 μm away from electrode 1. The solid line is recorded voltage; dotted lines at the beginning and end of the step indicate voltage applied to electrode 1. At a nominal holding potential of −50 mV, electrode 1 applied −48.72 mV (V1) and electrode 2 recorded −51.23 mV (V2). The difference of 2.51 mV is due to differences in the offset in amplifier. At +10 mV command, V1 = +9.87 mV, V2 (bottom trace, solid line) is +9.83 mV (+7.32 mV observed + 2.51-mV offset correction). After some tests and some increase in series resistance, for nominal 40-mV depolarization (to −10 mV), V1 = 39.55 mV, V2 = 38.9 mV for V2/V1 of 0.96. For a nominal 60-mV depolarization (to +10 mV), V1 = 58.59 mV, V2 = 57.13 for V2/V1 of 0.98. Note that recorded voltage at V2 reached applied voltage at V1 within 400 μs, and that in steady state they coincide. Cell capacitance was 43.0 pF. $[Ca^{2+}]_o$ = 3 mM (solution C).

Charge-carrier and I-V relations. Figs. 6 and 7 show evidence bearing on the nature of the inward current. Fig. 6 shows typical current records of a single cell taken in $[Ca^{2+}]_o$ = 3 mM and again in 30 mM, as well as the *I-V* relations of the peak currents. Among many cells studied while in $[Ca^{2+}]_o$ = 3 mM, with results similar to the cell shown in Fig. 6, activation of inward current was first found between −30 and −20 mV; maximum current occurred between +10 and +20 mV; the reversal potential was ~ +75 mV. The maximum current varied from cell to cell, in part because of variations in cell sizes and in part because of differences in the quality of the individual cells. For seven good quality cells, knowing the total capacitance of

each cell, and assuming a specific membrane capacitance of 1.15 $\mu F/cm^2$, the density of the inward current when $[Ca^{2+}]_o$ = 3 mM is estimated to be 19.5 ± 2.1 $\mu A/cm^2$. This value is in good agreement with that of the myocytes of the urinary bladder (20 $\mu A/cm^2$, Klöckner and Isenberg, 1985*b*), and thrice that of the rabbit ileal muscle (6.3 $\mu A/cm^2$, Ohya et al., 1986).

Increased $[Ca^{2+}]_o$. As illustrated in Fig. 6, when $[Ca^{2+}]_o$ was increased from 3 to 30 mM, the peak inward current was nearly doubled. Activation was shifted towards more positive voltages and the reversal potential was shifted to >90 mV (94 mV extrapolated). The shift in the reversal potential of this cell was +25 mV; the

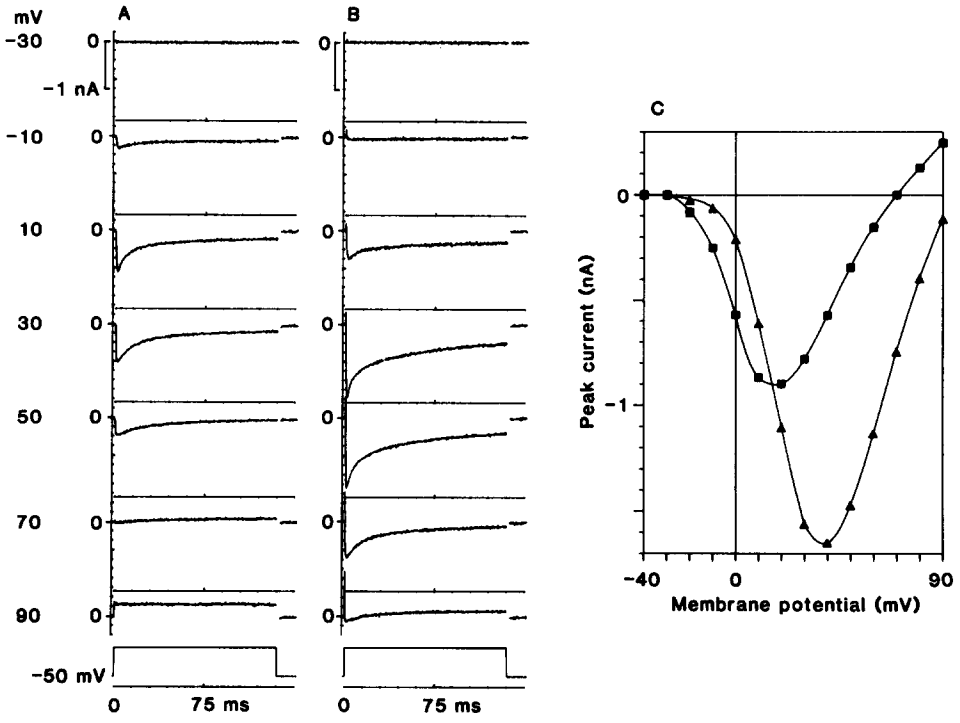

FIGURE 6. Effect of increasing $[Ca^{2+}]_o$ on Ca^{2+} current. Cell capacitance, 48.5 pF. (*A* and *B*) Actual currents in 3 mM Ca^{2+} (*A*, solution F, Table I) and 30 mM Ca^{2+} (*B*, solution G). By comparing traces in *A* and *B*, it can be seen that in 30 mM Ca^{2+}, activation is shifted towards more positive voltages, current maximum is markedly increased, and voltage at which it is reached shifted to more positive levels. Reversal potential is more positive than +90 mV. (C) *I-V* relations. Squares, 3 mM Ca^{2+}; triangles, 30 mM Ca^{2+}. Note the shift of the curve along the voltage axis, and the marked increase of current in 30 mM Ca^{2+}.

expected shift of E_{Ca} was 30 mV. In three other cells, similar shifts were observed, although the actual amount was not nearly as close to the expected shift of E_{Ca}. The shortfall can be attributed partly to an imperfect selectivity to Ca^{2+} (see Discussion), or to difficulties in determining E_{Ca} (Hagiwara and Byerly, 1981).

The rightward shift of the activation of the inward current is to be explained by the effect of high Ca^{2+} on the surface negative charges (Frankenhaeuser and Hodg-

kin, 1957), through both a screening and a binding effect (McLaughlin et al., 1971) that tend to make the potential difference within the membrane somewhat less steep than might be expected from the overall membrane potential difference. It is interesting to note that in another experiment (not shown) where 3 and 30 mM of Ba^{2+} were used on the same cell in place of Ca^{2+}, the rightward shift was significantly less. This observation is in agreement with that previously made on the multicellular preparation (Inomata and Kao, 1985), and is to be explained by the reasoning that

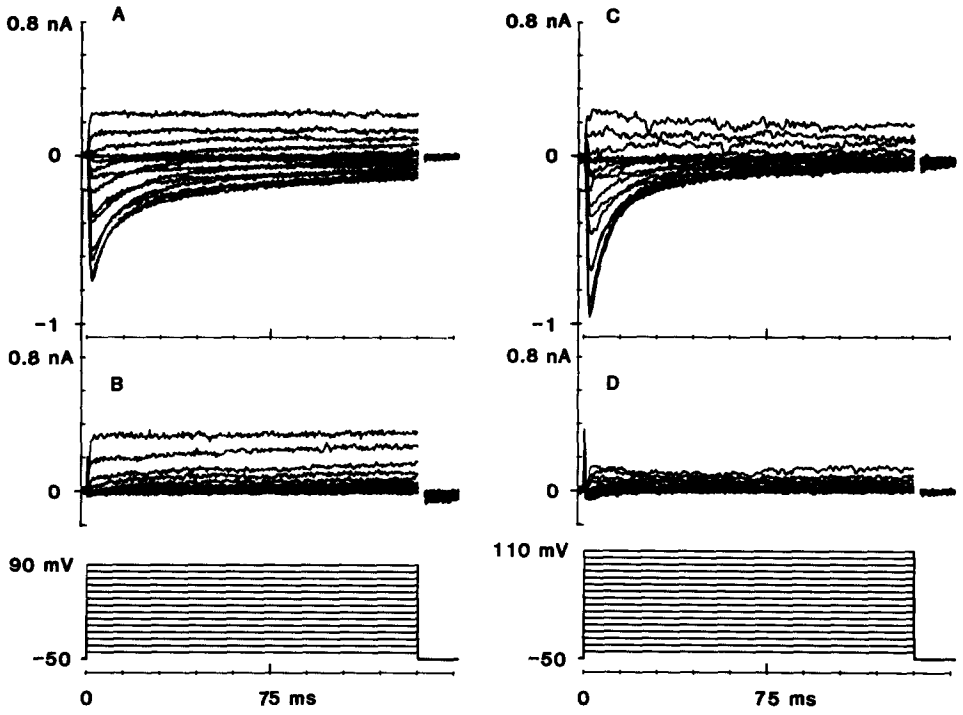

FIGURE 7. Effects of reducing $[Ca^{2+}]_o$ and of Co^{2+} on I_{Ca}. Holding potential, −50 mV; depolarized in 10-mV increments to +90 mV in *A* and *B*, and to +110 mV in *C* and *D*. *A* and *B* are from one cell with capacitance of 37.2 pF. (*A*) in 3 mM Ca^{2+} (solution F); (*B*) in Ca^{2+}-free medium (solution E). Note total absence of any inward current, even though the medium contained 105 mM Na^+. Also note that outward currents appear at lower depolarization in *B* than in *A*, and that for the same voltage, outward current is larger in *B* than in *A*. Outward current is due to an efflux of Cs^+ through Ca^{2+} channel (see Discussion). (*C* and *D*) In another cell the capacitance was 49.2 pF. (*C*) in 3 mM Ca^{2+} (solution F), (*D*) in 3 mM Ca^{2+} and 5 mM Co^{2+} (solution F with added $CoCl_2$). Inward current is blocked, and outward current appreciably reduced, supporting the conclusion on Cs^+ efflux through the Ca^{2+} channel.

Ba^{2+} had primarily a screening effect on the surface negative charges, and little binding tendency (McLaughlin et al., 1971).

Reduced $[Ca^{2+}]_o$ and Co^{2+}. Fig. 7 shows some typical current records when $[Ca^{2+}]_o$ was reduced or when Co^{2+} was used. Whereas inward current of one cell was completely abolished in a nominally Ca^{2+}-free medium, the outward current not

only persisted but also increased, especially upon large depolarizations (Fig. 7 *B*). In 5 mM of Co^{2+} the inward current of another cell was completely blocked, but on large depolarizations, some outward currents remained (Fig. 7 *D*) that were significantly smaller than those before Co^{2+} (Fig. 7 *C*).

Since the potassium channel had been blocked by the use of Cs^+, and in view of the very low intracellular Ca^{2+} and the very large chemical gradient of Ca^{2+}, a possible explanation of these outward currents is that intracellular K^+ or possibly Cs^+

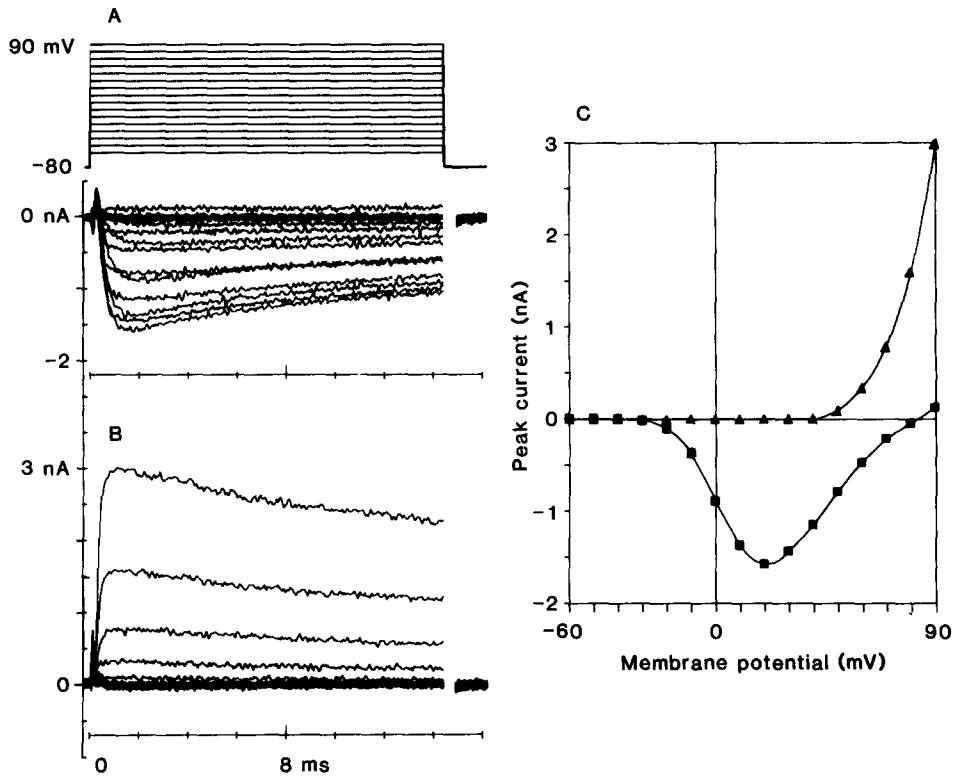

FIGURE 8. Effect of Ca^{2+}-free solution on taenia myocyte. Cell capacitance, 52.7 pF; temperature 33.8°C; holding potential, −80 mV (more negative than usual −50 mV); depolarized in 10-mV increments to +90 mV in both *A* and *B*. Note fast time scale. (*A*) in 3 mM Ca^{2+} (solution F), showing inward current, and small outward current at voltages positive to reversal potential. (*B*) in Ca^{2+}-free solution (solution E). Inward current is lost, but outward current markedly increased. (*C*) *I-V* relations, squares represent 3 mM Ca^{2+} (*A*) and triangles represent Ca^{2+}-free solution (*B*).

from the pipette solution was moving outwards through the Ca^{2+} channel (see also Fenwick et al., 1982; Lee and Tsien, 1982), hence their reduction in Co^{2+}.

The outward current under Ca^{2+}-free conditions is further examined at a holding potential of −80 mV (Fig. 8). One taenia cell was first subjected to depolarizing steps when in $[Ca^{2+}]_o$ = 3 mM (Fig. 8 *A*, and square symbols in *C*). Activation occurred close to −30 mV; maximum inward current occurred at +20 mV; and the

reversal potential was +81 mV. The outward current was small, ~0.1 nA at +90 mV (Fig. 8 *A*). In a nominally Ca^{2+}-free solution, there was no inward current, but the outward current became much larger than that observed when in Ca^{2+} (Fig. 8 *B*, and triangles in *C*). Outward current became apparent at +50 mV, as contrasted with +81 mV in Ca^{2+}. It could have started at even less positive voltages, if there were no trace amounts of Ca^{2+} in the bath solution that might have interfered with the mobility of Cs^+ through the Ca^{2+} channel (see Hess et al., 1986).

Absence of Na^+ current. An important detail in Figs. 7 *B* and 8 *B* that merits attention is the absence of any inward current in a nominally Ca^{2+}-free solution. The bath solution contained 105 mM Na^+. In very low $[Ca^{2+}]_o$ with EGTA, the Ca^{2+} channel in the guinea pig urinary bladder smooth muscle is permeable to Na^+ (Klöckner and Isenberg, 1985*b*). Also, in a vascular smooth muscle cell, which usually exhibits a Ca^{2+} channel, a Na^+ channel blockable by high concentrations of

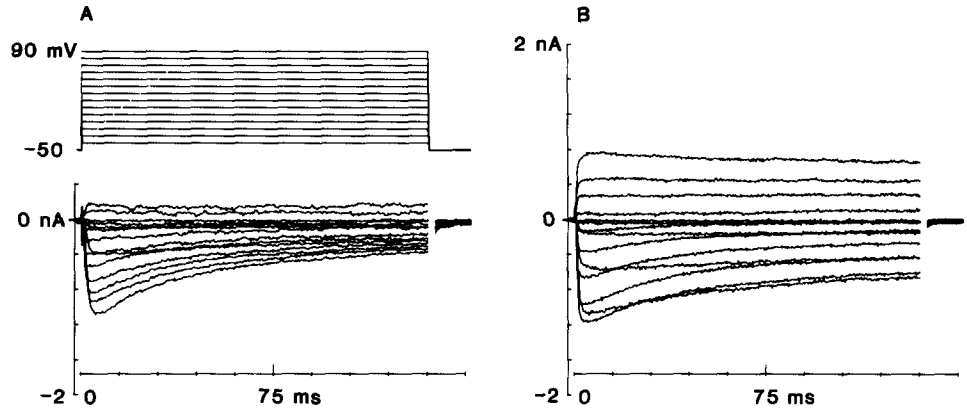

FIGURE 9. Sr^{2+} and Ba^{2+} currents through Ca^{2+} channels of taenia cells. Bath solutions are modified solution F, with 3 mM of Ca^{2+} replaced by equimolar concentrations of Sr^{2+} or Ba^{2+}. (*A*) Sr^{2+}: cell capacitance, 62.0 pF. Voltage protocol is shown on top. Note prolonged inward current. (*B*) Ba^{2+}: cell capacitance 62.1 pF. Inward current is more prolonged than in Sr^{2+}, and outward current is prominent.

tetrodotoxin can be unmasked by a highly negative holding potential (Sturek and Hermsmeyer, 1986). The absence of any inward current in the taenia myocytes held at −50 or −80 mV indicates that Na^+ influx plays no role in the inward current, a point which has been deduced from studies on multicellular preparations (Inomata and Kao, 1976). Quite possibly, under the conditions of the present experiments, the trace amount of Ca^{2+} in the nominally Ca^{2+}-free solution was sufficient to prevent the type of Na^+ permeability seen in the bladder myocytes. If this explanation were plausible, then in the physiological range of $[Ca^{2+}]_o$, there surely would be no Na^+ contribution to the fast inward current.

Sr^{2+} and Ba^{2+}. Fig. 9 shows that these alkaline earth divalent cations are capable of carrying the inward current through the Ca^{2+} channel. In each case, the usual 3 mM Ca^{2+} was replaced by either Sr^{2+} (Fig. 9 *A*) or Ba^{2+} (Fig. 9 *B*). Although Sr^{2+} resembles Ca^{2+} in many respects, the inward current inactivates appreciably more

slowly than I_{Ca}. This feature is even more exaggerated in the case of Ba^{2+}. In addition, the outward current in Ba^{2+} is significantly larger than in Ca^{2+}. The main features of these observations have been described on the multicellular preparation (Inomata and Kao, 1979, 1985).

Activation of I_{Ca}. Fig. 10 shows the voltage-conductance relation in two concentrations of Ca^{2+}. When $[Ca^{2+}]_o$ = 3 mM, inward current above noise level was first detectable at ~−30 mV. Half-activation was reached at −1 mV and full activation at +35 mV. When $[Ca^{2+}]_o$ = 30 mM, the activation curve is shifted towards more positive voltages by ~20 mV. Activation occurred first at ~−10 mV. Half-activation

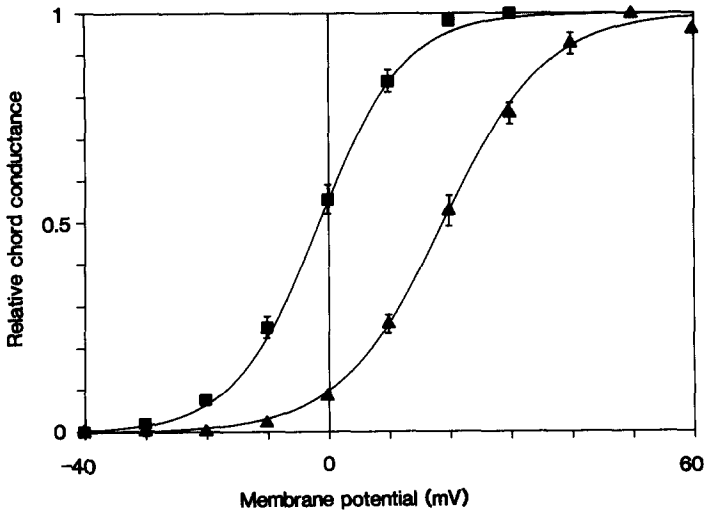

FIGURE 10. Steady-state activation of Ca^{2+} current. Square symbols for seven cells in 3 mM Ca^{2+} (solution F); triangles for four cells in 30 mM Ca^{2+} (solution G). Values are means; vertical bars represent SEM, if larger than symbols. Chord conductance at different voltages are normalized to that at either +30 mV (for 3 mM Ca^{2+}) or +50 mV (for 30 mM Ca^{2+}). In two cells in 30 mM Ca^{2+}, current did not reverse direction even at the highest depolarization. In these cases, reversal potential was based on extrapolated value. Solid curves are described by:

$$y = \{1 + \exp[(V + 1.5\text{ mV})/-7\text{ mV}]\}^{-1} \text{ in 3 mM } Ca^{2+}, \text{ and}$$

$$y = \{1 + \exp[(V - 18.8\text{ mV})/-8.5\text{ mV}]\}^{-1} \text{ in 30 mM } Ca^{2+}.$$

was now at +19 mV, and full-activation at ~+60 mV. The positive shift of the curve in the higher Ca^{2+} concentration is to be explained by an effect on the negative surface charge (Frankenhaeuser and Hodgkin, 1957).

In some other cells, multiple forms of Ca^{2+} channel have been recognized through their different activation characteristics (for review see McCleskey et al., 1986). In the taenia myocytes, it has not been possible to use such maneuvers to distinguish clearly different forms of Ca^{2+} channels. This feature is illustrated in Fig. 11, which shows that in one taenia myocyte, the only significant difference between holding at −80 mV from holding at −30 mV is the magnitude of the I_{Ca}. However,

multiple forms of Ca^{2+} channel can possibly be recognized by differences in their inactivating properties (see below).

Kinetics of activation. The kinetics of activation in Ca^{2+} can be approximated by m^4 kinetics, with a time constant of 0.47 ms in both Ca^{2+} and Ba^{2+}. The fit was better in Ba^{2+}, probably because the inactivation was considerably slower and posed less of an interference with the curve-fitting. Nevertheless, it should be recalled that our voltage control is only fully reliable after the first 400 μs. So, the kinetics of activation is really too fast for us to study with confidence.

Deactivation of I_{Ca}. When I_{Ca} was turned off at its peak, the tail current declined very rapidly. These measurements were attempted only in a few cells, because the process was too rapid for our present capability. All that can be said is that I_{Ca} declined almost fully in <1 ms.

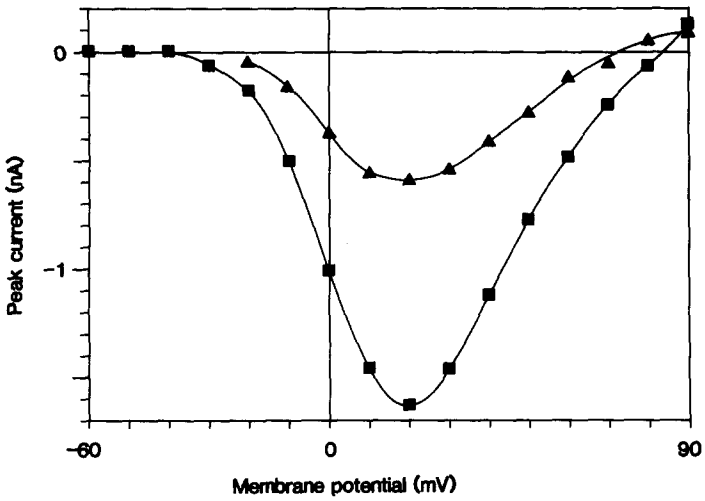

FIGURE 11. Effect of holding potential on current-voltage relations of peak Ca^{2+} current. Cell capacitance, 52.8 pF. $[Ca^{2+}]_o$ = 3 mM (solution F). Square symbols, holding potential −80 mV; triangles, holding potential −30 mV. Multiple forms of Ca^{2+} channel in taenia myocytes could not be demonstrated by differences in activation properties. See text for more details.

Inactivation

Kinetics of inactivation. When a depolarizing voltage step is maintained, I_{Ca} declined after reaching a maximum (Fig. 12 *A*). The decline is nearly complete in 2 s. The time course of this inactivation is complex, consisting of three exponential terms (Fig. 12 *B*). Both the magnitude and the time constant of decay of each component are influenced by membrane potential (Fig. 12, *C* and *D*). The voltage dependence of these properties of the fast component differs quite distinctly from those of the two slower components. The decay becomes slower (i.e., the time constant of decay increases) with more positive voltages (Fig. 12 *C*). The magnitude of the fast component is much more sensitive to voltage than the two slower compo-

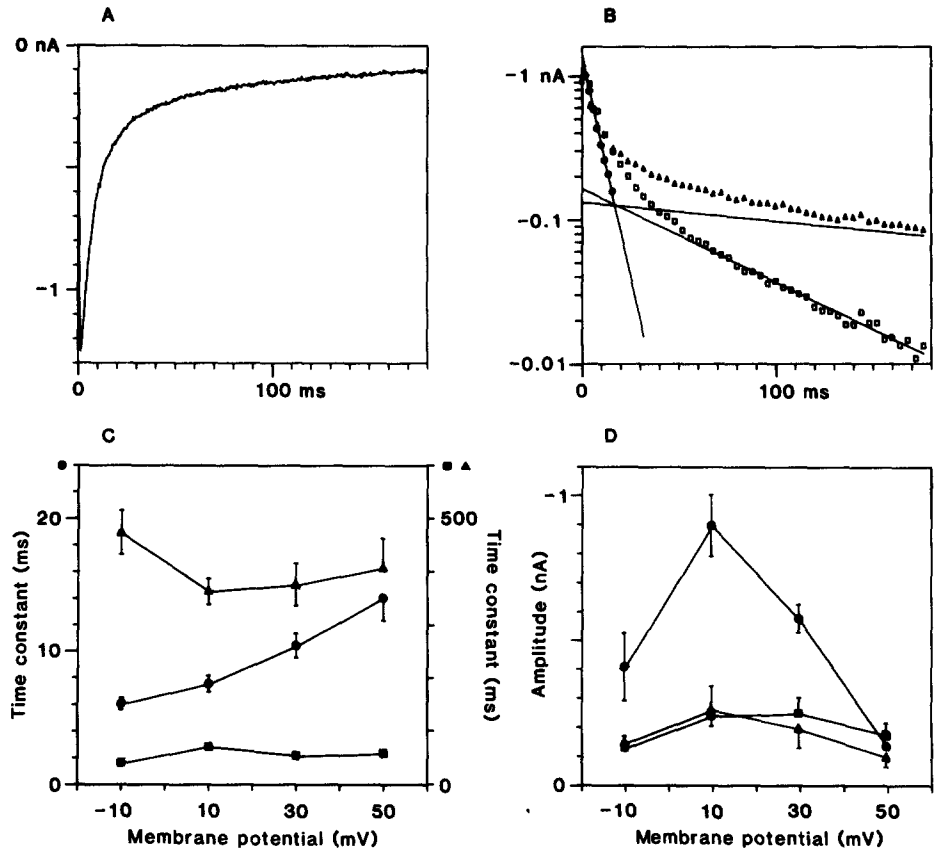

FIGURE 12. Inactivation of Ca^{2+} current. Cell capacitance 46.0 pF. $[Ca^{2+}]_o$ = 3 mM (solution F). (*A*) Ca^{2+} current induced by stepping voltage to +10 mV from a holding potential of −50 mV. (*B*) Inactivation time course plotted on semilogarithmic coordinates, showing three components of exponential decay (filled circles, fast component; squares, middle component; triangles, slow component). Fit: $-I_{Ca} = 1.37 \exp(-t/7.15) + 0.164 \exp(-t/66.84) + 0.132 \exp(-t/326.78)$. Actual fitting of fast component was done using a recording at a higher sampling rate; fitting of slow component was done using a longer depolarization (1.8 s, at the end of which I_{Ca} is completely inactivated). (*C*) Effect of membrane potential on time constants of inactivation of individual components (circles, fast; squares, middle; triangles, slow). Data from five different cells in 3 mM Ca^{2+}. Symbols represent means ± SEM. Ordinate on the left is for the fast component, as indicated at top; ordinate on the right is for the other two components. Individual means at −10, +10, +30, and +50 mV, respectively are: 6, 8, 10, and 14 ms for fast component; 40, 71, 54, and 58 ms for middle component; and 473, 364, 375, and 407 ms for slow component. Note the different voltage dependence of different components. (*D*) Effect of membrane potential on amplitude of individual components. Data from five different cells (identifying symbols as before). Amplitude is determined from extrapolated intercept on ordinate in curves similar to those shown in *B*. Note different voltage dependence of different components.

nents. Thus, it has an inverted V-shape with a sharp maximum at +10 mV and declines at more positive and more negative voltages (Fig. 12 *D*).

The voltage dependence of the magnitude of the two slower components are rather similar to each other, with differences appearing only with rather positive voltages. For the middle component, a small maximum is seen at +30 mV, but for the slower component, the maximum is seen at +10 mV (Fig. 12 *D*). However, the two slower components can be distinguished from each other by a four to fivefold difference in their rates of decay, and by the different influences of voltage on such rates. The rate of decline of the middle component has a very shallow inverted V-shape, with a time constant of 71.0 ms at +10 mV, 40 ms at −10 mV, and 54 and 58 ms at +30 and +50 mV, respectively. The voltage dependence of the decay of the slow component has a shallow and skewed V-shape, with a time constant of

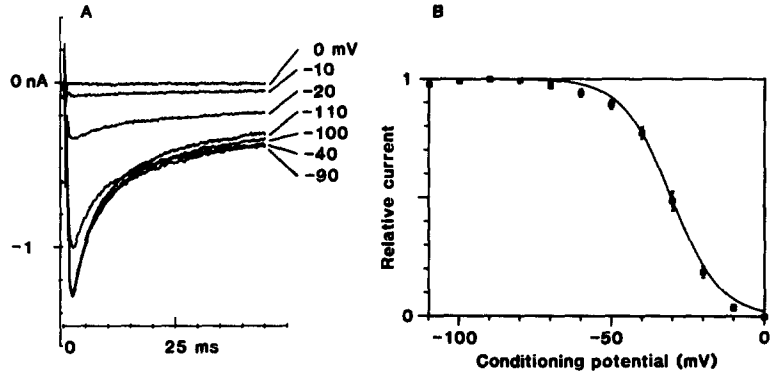

FIGURE 13. Steady-state inactivation of Ca^{2+} current in 3 mM Ca^{2+}. (*A*) Ca^{2+} current was activated by stepping to +10 mV, from preceding conditioning pulse of 5-s duration of various voltages (−110 to 0 mV). Current during the conditioning pulse is not shown. Current attributed to each conditioning step is identified by a label at the right end of trace. For clarity, some traces have been omitted from the record, but values are included in the plot in *B*. (*B*) Relative current vs. conditioning voltage. Results from seven cells, means ± SEM. Peak currents of each cell are scaled so that the value at the −90-mV conditioning voltage is 1.0. Smooth curve: $y = \{1 + \exp[(V + 30.4\text{ mV})/8\text{ mV}]\}^{-1}$.

decay averaging 364 ms at +10 mV, 473 ms at −10 mV, 375 ms at +30 mV, and 407 ms at +50 mV (Fig. 12 *C*).

Three inactivating components persisted in Ba^{2+} solution (3 mM), and their time constants were about five times larger than those in Ca^{2+} solution (Yamamoto et al., 1988).

Steady-state inactivation. Fig. 13 summarizes the studies on the steady-state inactivation of the I_{Ca}. In eight cells, held at −50 mV, maximum I_{Ca} was elicited by depolarizing to +10 mV (test pulse, V2, 45-ms duration). A conditioning pulse (V1) of 5 s was applied immediately before the test pulse, varying in amplitude from −110 to 0 mV. In another group of cells (not shown), similar tests were made with V1 lasting 1.25 s. The inactivation curve of 5 s is virtually the same as that for V1.

The steady-state inactivation curve is sigmoidal, following the classical Hodgkin-Huxley form. The data are fitted well by a curve described by the function $y =$

$\{1 + \exp[(V + 30.4\ mV)/8\ mV]\}^{-1}$, where -30.4 mV is the voltage at which I_{Ca} is reduced to half ($V_{0.5}$), and 8 mV is the slope. For the series with a 1.25-s conditioning step, $V_{0.5}$ is -29 mV and the slope is 7 mV. These values can be compared with a $V_{0.5}$ of -43 mV and a slope of 6 mV in the guinea pig bladder smooth muscle (Klöckner and Isenberg, 1985*b*), and a $V_{0.5}$ of -56 mV and a slope of 10 mV in the toad stomach smooth muscle (Walsh and Singer, 1987). It should be noted that in the taenia myocytes at the usual holding potential of -50 mV (which is also the usual resting potential reported in the literature), 90% of the Ca^{2+} channels are available.

Steady-state inactivation of the individual components. Fig. 14 summarizes the steady-state inactivation properties of the three different components of the I_{Ca}. The magnitude of the fast-decaying component is affected differently by the conditioning voltage from that of either the middle-decaying or the slow-decaying components (Fig. 14 *A*). The h_∞ curves (Fig. 14 *B*) shows that for the fast component, $V_{0.5}$ is -35.6 mV with a slope factor of 7 mV. For the middle component, $V_{0.5}$ is -26.3 mV and the slope factor 5 mV. For the slow component, $V_{0.5}$ is -23.8 mV and the slope factor is 5 mV. Thus, the steady-state inactivation relation of the overall I_{Ca} shown in Fig. 13, with a $V_{0.5}$ of -30 mV must represent a composite of the three components, with the slope factor of the fast component dominating. The time constant of decay of each component is relatively unaffected by the conditioning voltage (Fig. 14 *C*).

Recovery from inactivation. The question of how rapidly I_{Ca} can recover to permit a subsequent I_{Ca} to develop has been examined by using two-pulse protocols (Fig. 15). In the results shown in Fig. 15 *A*, the conditioning pulse (V1) was 2 s long to inactivate all components of I_{Ca}, and the test pulse (V2) was 45 ms. From four different holding potentials, V1 and V2 reached the same voltage (+10 mV). The interval separating V1 and V2 was varied. In spite of some variations from cell to cell and a complex kinetics with multiple exponential terms, half-recovery occurred between 480 ms to 1 s after V1. The more negative the holding potential, the faster was the recovery.

For the results shown in Fig. 15 *B*, V1 was only 5 ms, a duration which would have inactivated about half of the fast component and <10% of the other two components. By this protocol, the recovery of the fast component can be selectively estimated. The curves, readily fitted with a single exponential of time constant 71.6 ms, show that regardless of the holding potential, half-recovery of the fast component can occur in slightly over 40 ms after a prior depolarization. This rate of recovery is clearly more closely associated with the frequency of repetitive spikes in a burst of action potentials (see Fig. 2).

Ramp clamp. The success in blocking I_K in these dispersed myocytes provides an opportunity to estimate the influx of Ca^{2+} during a depolarization episode. A voltage-command waveform was structured to resemble that of the action potential in 3 mM Ca^{2+} (Fig. 3 *B*), and then used to elicit I_{Ca} in a voltage-clamp run. Fig. 16 illustrates one of these experiments. The I_{Ca} produced by the ramp voltage-command was double peaked, because maximum I_{Ca} was obtained at +10 to +20 mV, a level which was attained on both the ascending and the descending phases of the ramp command. By integrating the current-time area, the charge moved was found to be 9.02 pC, equivalent to 0.05 fM of Ca^{2+}. If all this amount were distributed

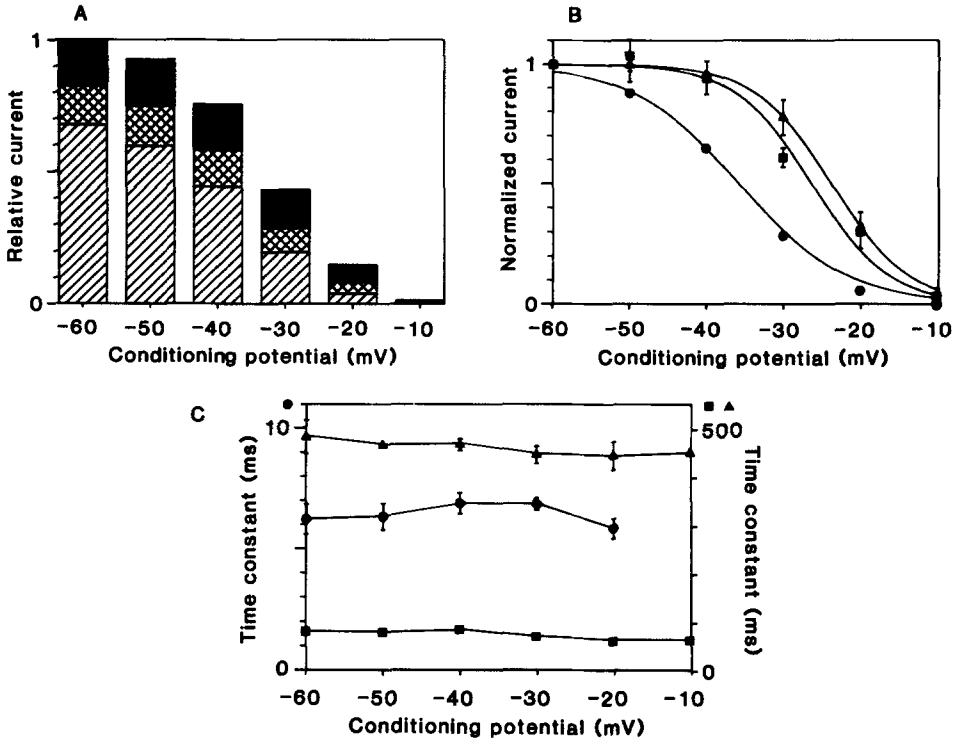

FIGURE 14. Steady-state inactivation of three differently inactivating components of Ca^{2+} current. $[Ca^{2+}]_o$ = 3 mM. The inactivating time course of Ca^{2+} current induced by stepping to +10 mV from a preceding 5-s conditioning step of various voltages (−60 to −10 mV) was analyzed by the procedure shown in Fig. 12. Averaged amplitudes (*A* and *B*) and time constants (*C*) of three cells. (*A*) Fractional contribution of individual components to the compound steady-state inactivation relation is shown in Fig. 16. Hatched bar, fast component; cross-hatched bar, middle component; filled bar, slow component. Amplitudes have been scaled so that the sum of three components would be 1.0 at −60-mV conditioning voltage in each individual cell. (*B*) Steady-state inactivation of individual components (circles, fast; squares, middle; triangles, slow). Amplitude was normalized so that the value of each component at −60 mV would be 1.0 in each individual cell. Data points are means ± SEM. Smooth curves are fitted to:

$$\text{fast, } y = \{1 + \exp[(V + 35.8\text{ mV})/7\text{ mV}]\}^{-1}$$

$$\text{middle, } y = \{1 + \exp[(V + 26.3\text{ mV})/5\text{ mV}]\}^{-1}$$

$$\text{slow, } y = \{1 + \exp[(V + 23.8\text{ mV})/5\text{ mV}]\}^{-1}.$$

(*C*) Time constant of inactivation of individual components vs. conditioning voltage. Symbol identities same as before. Ordinate on left for fast component, and ordinate on right for the other two components, as indicated by symbols at top.

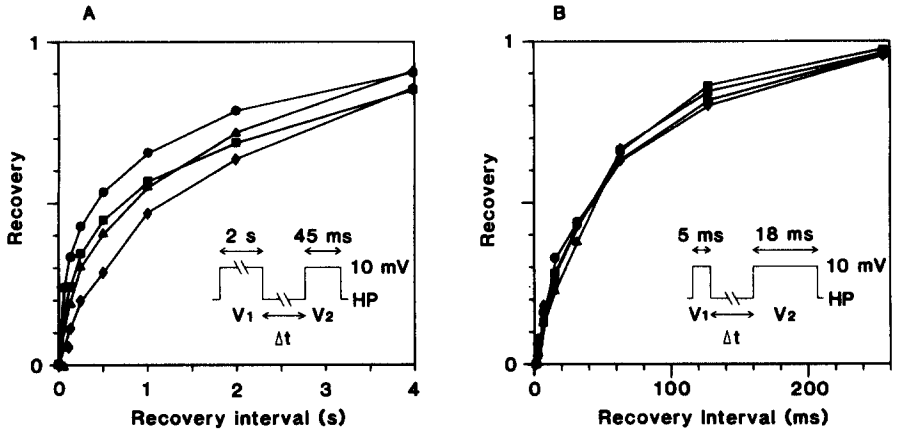

FIGURE 15. Recovery of Ca^{2+} current from inactivation. Two-pulse protocol as indicated in insets. Current due to V2 as a fraction of current due to V1 (ordinate) is plotted against the intervals between voltage steps (abscissa). $[Ca^{2+}]_o$ = 3 mM (solution F). (*A*) Overall recovery; duration of V1 (2 s) was long enough to inactivate all three components. Cell capacitance, 62.4 pF. Holding potentials: −90 mV (circles), −70 mV (squares), −50 mV (triangles), and −30 mV (diamonds). (*B*) Recovery of fast component; V1, of 5-ms duration, inactivated ~50% of fast component and <10% of other two components. Since the fast component is dominant, recovery of fast component could be examined with this voltage protocol. Holding potentials: −110 mV (diamonds), −90 mV (circles), −70 mV (squares), and −50 mV (triangles). Data points are means of seven cells. Ordinate was scaled such that no recovery occurred at the minimum interval (2 ms). When averaged, the time course can be fitted with a single exponential with a time constant of 71.6 ms.

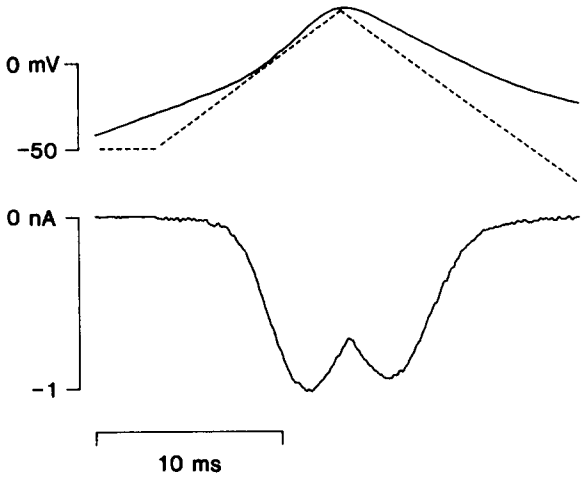

FIGURE 16. Ca^{2+} current during a ramp clamp. $[Ca^{2+}]_o$ = 3 mM (solution F). Top trace, solid curve represents the action potential elicited by a brief current pulse (same recording as shown in Fig. 3 *B*). Middle trace, broken line is a ramp-clamp pulse generated to mimic action potential. Bottom trace (solid line) is Ca^{2+} current of different taenia cells subjected to ramp clamp as shown above. Cell capacitance, 52.8 pF; temperature, 32°C. The current has two minima because maximum Ca^{2+} current is observed ~+10 mV, and ramp-clamp reaches this voltage twice, once on the rising phase and a second time on the falling phase. Integration of the area under the current trace shows that 9.02 pC of electric charge entered the cell during the process. See text for further comments.

homogeneously throughout the cell volume of 6 pl (average cell volume), the intracellular [Ca^{2+}] could rise to 8 μM.

DISCUSSION

Comparison with Other Work

Earlier voltage-clamp studies on multicellular preparations were beset with problems arising primarily from the series resistance. As a result, only limited qualitative conclusions could be drawn. With respect to the early transient inward current, these qualitative conclusions included: (*a*) the inward current in the taenia coli was carried by Ca^{2+} (Inomata and Kao, 1976), (*b*) Sr^{2+} and Ba^{2+} could also pass through this channel, with greater ease than Ca^{2+}, but the rate of inactivation was slower than that for Ca^{2+} (Inomata and Kao, 1979, 1985), and (*c*) depolarization induced inactivation of I_{Ca}, with half-inactivation occurring at ~ -30 mV (Inomata and Kao, 1979). All these conclusions, unknown until those multicellular studies, have now been confirmed by the present results on the single myocyte (see also Ohya et al., 1986 on rabbit ileal "smooth muscle balls"). It is ironic that were it not for the present ability to introduce Cs^{2+} directly to the cell interior, overlap of inward and outward currents would be as much a problem in the single cell (Fig. 2) as it was in multicellular preparations. In perspective, therefore, much of the criticisms of multicellular work generically (e.g., Bolton et al., 1981) were exaggerated because they were based more on general anticipated fears rather than on specific instances of failure. Nevertheless, the multicellular studies could not provide any information on the kinetics of activation, deactivation, or inactivation of I_{Ca}. Nor was it possible to completely separate the inward and outward currents from each other for detailed study of the individual currents.

Compared with other recent studies on single cells of smooth muscles, there are some significant differences in our results from those of other investigators. It should be emphasized that almost all the present data were obtained in media containing the physiological concentration of Ca^{2+} (3 mM). With the exception of the work of Klöckner and Isenberg (1985*a*, *b*) and of Ganitkevitch et al., (1986), all other studies whether on amphibian cells (Caffrey et al., 1980, 1986; Walsh and Singer, 1981, 1987) or mammalian cells (Bean et al., 1986; Droogmans and Callewaert, 1986 (Sturek and Hermsmeyer, 1986) were conducted in bathing solutions containing either an elevated concentration of Ca^{2+}, or Ba^{2+}. Although these procedures facilitated the recording of the inward current, they do produce complex effects beyond an innocent increase in the driving force on Ca^{2+}, or a simple prolongation of the I_{Ca}. The activation and inactivation processes in the Ca^{2+} channel can be markedly affected by such procedures (see Inomata and Kao, 1979, 1985; Ohya et al., 1986), and some caution should be exercised in extrapolating the derived data to normal physiological phenomena.

A major distinguishing feature of the present results is the high current density of the single taenia myocyte (19.5 $\mu A/cm^2$; contrast with that of Ganitkevitch et al., 1986 on the same cell, and Ohya et al., 1986 on a different intestinal muscle cell). Perhaps the density of the Ca^{2+} channels in the guinea pig taenia myocyte is higher than that in either amphibian smooth muscles or in mammalian vascular smooth

muscles, and that the observed current density reflects that property. However, we suspect that our results are due in no small measure to the use of the "KB" medium (Isenberg and Klöckner, 1982) in the preparation of our cells, as Klöckner and Isenberg (1985*a*, *b*) were the only other investigators to have observed similar current densities in the urinary bladder myocytes (20 $\mu A/cm^2$). Possibly, for the same reason, "run-down" of the I_{Ca} was not a serious and limiting problem in our study. It should also be recalled that our cells could be space clamped very well in their elongated and relaxed state (Fig. 5), and that we had no need to use shortened cell fragments to obtain spatial voltage uniformity (Ohya et al., 1986).

Ganitkevitch et al. (1986, 1987) also studied the whole-cell current of the guinea pig taenia coli, but their results and ours differ significantly in a number of ways. The main differences are: (*a*) although they also observed more than one component in the kinetics of inactivation, their fast component corresponded to our middle component with a time constant of ~45 ms. Their slow component was in agreement with our slow component. They did not observe another component corresponding to our fast component which had a time constant of decay of ~7 ms. (*b*) Their inward current never inactivated completely even with depolarizing steps of many seconds, whereas ours did within 2 s. (*c*) Their h_∞ curve had a U-shape, with availability of the Ca^{2+} channels decreasing towards a minimum but finite value at around +20 mV, but again increasing with more positive voltages. Our h_∞ curves, whether for all three components combined or for each individual component, followed the Boltzman distribution, and declined to zero at ~−10–0 mV.

We cannot explain such major differences, but such differences do impact upon the interpretations of mechanisms underlying inactivation of the I_{Ca} (see below). One further difference is to be found in the rate of recovery from inactivation, but this difference can be attributed to differences in the voltage protocol used to study recovery. Ganitkevitch et al. (1987) used a 500-ms long pulse to elicit I_{Ca}. We consider this pulse too short to produce complete inactivation of all components of the I_{Ca}, but too long to inactivate only the fastest component (see our Fig. 16).

Selectivity of the Ca^{2+} Channel

In 3 mM Ca^{2+}, the I_{Ca} observed in the present study reversed its polarity at ~+75 mV, a value which is considerably less than the expected equilibrium potential of +260 mV ($[Ca^{2+}]_o$ = 3 mM; $[Ca^{2+}]_i = 10^{-8}$ M; temperature, 35°C). Since the K^+ channels have been blocked, the outward current at voltages positive to +75 mV is passing through the Ca^{2+} channel. In agreement with results found in a number of other cells (e.g., chromaffin cells, Fenwick et al., 1982; ventricular myocyte, Lee and Tsien, 1982), the most likely charge carrier of this outward current is Cs^{2+} from the pipette solution. This conclusion is also consistent with some recent models of Ca^{2+} channel behavior, in which monovalent cations are viewed as readily mobile through the Ca^{2+} channel, except when at least one channel binding site is occupied by Ca^{2+} (Almers and McCleskey, 1984; Hess and Tsien, 1984). A similar movement of Na^+ through the Ca^{2+} channel of the smooth muscle cell of the guinea pig urinary bladder occurs in a Ca^{2+}-free and Mg^{2+}-free medium containing EGTA (Isenberg and

Klöckner, 1985), and in rabbit ileal muscle cells in low $[Ca^{2+}]_o$ conditions (Ohya et al., 1986).

Activation and Deactivation of I_{Ca}

Against a backdrop of past understanding that smooth muscles are often slower than other excitable tissues, the rate of activation of the I_{Ca} in single myocytes of the taenia is surprisingly fast, with maximum I_{Ca} attained in ~2 ms at 32–34°C. No part of this rapid activation is attributable to involvement of a Na^+ channel system, because we have excluded any I_{Na} in the taenia cell. Fast activation of I_{Ca} has also been observed in the smooth muscle cells of the guinea pig urinary bladder (Klöckner and Isenberg, 1985*b*).

Deactivation is also very fast, and the Ca^{2+} tail current disappeared completely within 1 ms of membrane repolarization. In the urinary bladder cells, Klöckner and Isenberg (1985*b*) reported that the Ca^{2+} tail currently deactivated within 2 ms after repolarization.

Inactivation

As shown in Results (e.g., Fig. 12), I_{Ca} in the taenia cell decreased and vanished completely within 2 s because of inactivation, even when depolarization was maintained. For Ca^{2+} channels, inactivation involves at least two possible mechanisms, a voltage-dependent inactivation (similar to that for Na^+ channels) and a $[Ca^{2+}]_i$-dependent inactivation (see e.g., Tsien, 1983). In some cells, inactivation is thought to be purely voltage dependent (*Neanthes* egg, Fox, 1981); in others, inactivation depends on the intracellular concentration of Ca^{2+} (*Paramecium*, Brehm and Eckert, 1978). In still others, inactivation is both voltage dependent and $[Ca^{2+}]_i$ dependent (calf cardiac Purkinje fibers and guinea pig ventricular myocytes, Lee et al., 1985). In the guinea pig taenia coli cells, Ganitkevitch et al., (1987) emphasized the major role of the $[Ca^{2+}]_i$-dependent component in the inactivation.

Our results suggest that inactivation in the taenia myocyte is influenced by both membrane voltage and $[Ca^{2+}]_i$. The observations supporting a voltage dependence are (*a*) at voltages negative to ~ -30 mV, when no inward I_{Ca} is detectable, some inactivation already exists which can be removed by hyperpolarization (Fig. 13); (*b*) in a Ca^{2+}-free solution where no Ca^{2+} influx occurs, the outward current through the Ca^{2+} channel still inactivates (Fig. 8 *B*); (*c*) the rate of recovery from inactivation is voltage-dependent when all inactivating components are examined together; and (*d*) in Fig. 14 *C*, when the voltage of the test-pulse was kept constant (+10 mV), the time-constant of the three inactivating components were nearly constant, even though the amplitude of the inward current varied widely because of different conditioning voltage steps.

The observations supporting a $[Ca^{2+}]_i$ dependence of inactivation are (*a*) when Ba^{2+} carried the inward current, the time course of all three inactivating components was much slowed, i.e., the nature of the influxing divalent cation influences inactivation; (*b*) the rate of recovery of the fast inactivating component from inactivation was voltage independent, and its time course was much slower than that of inactivation itself. In the voltage-dependent inactivation (Reuter, 1973), inactivation

and recovery from inactivation have the same time parameters. (*c*) The time course of the slowly inactivating components was faster when I_{Ca} was larger (Fig. 12 *C*), suggesting more direct relation to intracellular Ca^{2+} concentration.

In the present experiments, the intracellular Ca^{2+} concentration was kept well below the threshold for contraction (10^{-8} M, Obara and Yamada, 1984) by the inclusion of 1 mM EGTA in the pipette solution to improve the stability of recording. Under these conditions, one might question the relevance of the observations on the apparent Ca^{2+} dependence of inactivation. However, the rate of binding of Ca^{2+} to EGTA is relatively slow, and the immobilization of the influxed Ca^{2+} by EGTA could well lag behind the rate of entry of Ca^{2+} to allow some increase in $[Ca^{2+}]_i$ (Eckert and Chad, 1984). If the binding sites associated with a Ca^{2+}-dependent inactivation process were located near the inner end of the Ca^{2+} channel, then a transient increase in the concentration of Ca^{2+} in this region could be a distinct possibility, in spite of the presence of EGTA throughout the cell water.

Multiple Types of Ca^{2+} Channels

It is now clear that many cells have more than a single type of Ca^{2+} channels (see McCleskey et al., 1986). Among mammalian smooth muscle cells, those of the rat mesenteric artery (Bean et al., 1986) and of the primary culture from azygous vein of neonatal rats (Sturek and Hermsmeyer, 1986) have been shown to have two types of Ca^{2+} channels through whole-cell recordings. In the rabbit ear artery, single-channel recordings suggest the presence of two types of Ba^{2+}-conducting channels (20 and 8 pS, Aaronson et al., 1986).

In these smooth muscle cells as well as in cardiac myocytes (Bean, 1985; Nilius et al., 1985), the two types of Ca^{2+} channels are distinguished by their activation thresholds, current profiles, and inactivation characteristics. One type requires a negative holding potential (~ -80 mV) and relatively small depolarizations for activation; it inactivates within tens of milliseconds. The other type requires larger depolarizations and inactivates much more slowly. Using different holding potentials (usually -80 and -30 mV), the two types can be readily separated.

In the present experiments, the inactivation characteristics of the I_{Ca} suggest the existence of multiple forms of Ca^{2+} channels, but this possibility could not be confirmed by any peculiarities in activation properties. However, from single-channel recordings, at least two different types of Ca^{2+} channels have now been demonstrated in the taenia myocyte (Yamamoto et al., 1988). When carrying Ba^{2+} currents, one of these channels has a unit conductance of 21 pS, and the other 9 pS.

Possible Roles of Multiple Types of Ca^{2+} Channels

As shown in Results, the Ca^{2+} influx is entirely adequate to discharge the membrane capacity to produce the action potential. The fast-channel also inactivates fast enough to influence the repolarization phase of the action potential, although it may not be the only mechanism involved (see Yamamoto et al., 1989). Furthermore, the rate of recovery from inactivation of the fast-channel strongly influences the refractoriness of the taenia myocyte to repetitive action potential discharges. In support of the latter suggestion is the observation that in a burst of repetitive action

potentials, the interval between individual spikes is ~100 ms (corresponding to 10 spikes/s; e.g., Fig. 2), at which time ~75% of the I_{Ca} in the fast channel has recovered from a previous depolarization (Fig. 15). In any burst with a substantially higher rate of discharge, the height of each successive action potential tends to be lower than the preceding one, because of incomplete recovery.

In Results, it was estimated that during an action potential, the Ca^{2+} influx could potentially raise the intracellular Ca^{2+} concentration by 8 μM. Clearly, this is a gross overestimate based on the assumption that the influxed Ca^{2+} is distributed homogenously throughout the cell water. Such a situation is very unlikely to occur because of the presence of highly efficient intracellular Ca^{2+}-buffering systems. The main point of the estimate is to show that the fast Ca^{2+} channel is capable of supplying Ca^{2+} for contraction and other cellular processes.

The functions of the slow Ca^{2+} channel(s) are less obvious. They may be involved in pacemaking for automaticity, in modulating the generation of action potential by influencing the duration of bursts and discharges, in modulating or participating in responses to neurotransmitters, and possibly in some extended supply of Ca^{2+} for tonic contractions.

This work is supported by a grant from the National Institutes of Health (HD-00378).

We wish to thank the scientific liaison and management staff of the National Institute of Child Health and Human Development for all their help. We also wish to thank Drs. J. J. Singer and J. V. Walsh (University of Massachusetts Medical School) for helpful advice and comments in the early phase of our work, and Ms. Helen Krasnow for technical assistance.

Original version received 10 August 1987 and accepted version received 17 October 1988.

REFERENCES

Aaronson, P., C. D. Benham, T. B. Bolton, P. Hess, R. J. Lang, and R. W. Tsien. 1986. Two types of single-channel and whole-cell calcium or barium currents in single smooth muscle cells of rabbit ear artery and the effects of noradrenaline. *Journal of Physiology.* 377:36P. (Abstr.)

Almers, W., and E. W. McCleskey. 1984. Non-selective conductance in calcium channels of frog muscle: calcium selectivity in a single-file pore. *Journal of Physiology.* 353:585–608.

Bean, B. P. 1985. Two kinds of calcium channels in canine atrial cells. Differences in kinetics, selectivity, and pharmacology. *Journal of General Physiology.* 86:1–30.

Bean, B. P., M. Sturek, A. Puga, and K. Hermsmeyer. 1986. Calcium channels in muscle cells isolated from rat mesenteric arteries: modulation by dihydropyridine drugs. *Circulation Research.* 59:229–235.

Benham, C. D., and T. B. Bolton. 1983. Patch-clamp studies of slow potential-sensitive potassium channels in longitudinal smooth muscle cells of rabbit jejunum. *Journal of Physiology.* 340:469–486.

Benham, C. D., T. B. Bolton, R. J. Lang, and T. Takewaki. 1985. The mechanism of action of Ba^{2+} and TEA on single Ca^{2+}-activated K^+-channels in arterial and intestinal smooth muscle cell membranes. *Pflügers Archiv.* 403:120–127.

Bolton, T. B., T. Tomita, and G. Vassort. 1981. Voltage clamp and measurement of ionic conductance in smooth muscle. *In* Smooth Muscle: An Assessment of Current Knowledge. Chapter 2. E. Bülbring, A. F. Brading, A. W. Jones, and T. Tomita, editors. Edward Arnold, London.

Brehm, P., and R. Eckert. 1978. Calcium entry leads to inactivation of calcium channel in *Paramecium*. *Science*. 202:1203–1206.

Bülbring, E., A. F. Brading, A. W. Jones, and T. Tomita. 1981. Smooth Muscle. An Assessment of Current Knowledge. University of Texas Press, Austin, Texas. 563 pp.

Caffrey, J. M., N. C. Anderson, and J. W. Moore. 1980. Voltage clamp of single isolated smooth muscle cell. *Federation Proceedings*. 39:2077. (Abstr.)

Caffrey, J. M., I. R. Josephson, and A. M. Brown. 1986. Calcium channels of amphibian stomach and mammalian aorta smooth muscle cells. *Biophysical Journal*. 49:1237–1242.

Clapp, L. H., M. B. Vivaudou, J. V. Walsh, and J. J. Singer. 1987. Acetylcholine increases voltage-activated Ca^{2+} current in freshly dissociated smooth muscle cells. *Proceeding of the National Academy of Sciences*. 84:2092–2096.

Droogmans, G., and G. Callewaert. 1986. Ca^{2+}-channel current and its modification by the dihydropyridine agonist BAY K 8644 in isolated smooth muscle cells. *Pflügers Archiv*. 406:259–265.

Eckert, R., and J. E. Chad. 1984. Inactivation of Ca channels. *Progress in Biophysics and Molecular Biology*. 44:215–267.

Fenwick, E. M., A Marty, and E. Neher. 1982. Sodium and calcium channels in bovine chromaffin cells. *Journal of Physiology*. 331:599–635.

Fox, A. P. 1981. Voltage-dependent inactivation of a calcium channel. *Proceedings of the National Academy of Sciences*. 78:953–956.

Frankenhaeuser, B., and A. L. Hodgkin. 1957. The action of calcium on the electrical properties of squid axons. *Journal of Physiology*. 137:218–244.

Ganitkevitch, V. Ya., M. F. Shuba, and S. V. Smirnov. 1986. Potential-dependent calcium inward current in a single isolated smooth muscle cell of the guinea-pig taenia coli. *Journal of Physiology*. 380:1–16.

Ganitkevitch, V. Ya., M. F. Shuba, and S. V. Smirnov. 1987. Calcium-dependent inactivation of potential-dependent calcium inward current in an isolated guinea-pig smooth muscle cell. *Journal of Physiology*. 392:431–449.

Hagiwara, S., and L. Byerly. 1981. Calcium channel. *Annual Review of Neurosciences*. 4:69–125.

Hamill, O. P., A. Marty, E. Neher, B. Sakmann, and F. J. Sigworth. 1981. Improved patch-clamp techniques for high-resolution current recording from cells and cell-free membrane patches. *Pflügers Archiv*. 391:85–100.

Hess, P., J. B. Lansman, and R. W. Tsien. 1986. Calcium channel selectivity for divalent and monovalent cations. Voltage and concentration dependence of single channel current in ventricular heart cells. *Journal of General Physiology*. 88:293–319.

Hess, P., and R. W. Tsien. 1984. Mechanism of ion permeation through calcium channels. *Nature*. 309:453–456.

Hu, S. L., Y. Yamamoto, and C. Y. Kao. 1987*a*. Single channel basis of delayed rectification in dispersed cells of guinea pig taenia coli. *Biophysical Journal*. 51:200*a*. (Abstr.)

Hu, S. L., Y. Yamamoto, and C. Y. Kao. 1987*b*. Selectivity of the single delayed rectifier channel in smooth muscle cells of the guinea pig taenia coli. *Federation Proceedings*. 46:507. (Abstr.)

Inomata, H., and C. Y. Kao. 1976. Ionic currents in the guinea-pig taenia coli. *Journal of Physiology*. 255:347–378.

Inomata, H., and C. Y. Kao. 1979. Ionic mechanisms of repolarization in the guinea-pig taenia coli as revealed by the actions of strontium. *Journal of Physiology*. 297:443–462.

Inomata, H., and C. Y. Kao. 1985. Actions of Ba^{2+} on ionic currents of the guinea-pig taenia coli. *Journal of Pharmacology and Experimental Therapeutics*. 233:112–124.

Inoue, R., K. Okabe, K. Kitamura, and H. Kuriyama. 1986. A newly identified Ca^{2+}-dependent K^+

channel in the smooth muscle membrane of single cells dispersed from the rabbit portal vein. *Pflügers Archiv.* 406:138–143.

Isenberg, G., and U. Klöckner. 1982. Calcium tolerant ventricular myocytes prepared by preincubation in a "KB" medium. *Pflügers Archiv.* 395:6–18.

Isenberg, G., and U. Klöckner. 1985. Calcium currents of smooth muscle cells isolated from the urinary bladder of the guinea-pig: inactivation, conductance and selectivity is controlled by micromolar amounts of $[Ca]_o$. *Journal of Physiology.* 358:60P. (Abstr.)

Kao, C. Y., and J. R. McCullough. 1975. Ionic currents in the uterine smooth muscle. *Journal of Physiology.* 246:1–36.

Klöckner, U., and G. Isenberg. 1985*a*. Action potentials and net membrane currents of isolated smooth muscle cells (urinary bladder of the guinea pig). *Pflügers Archiv.* 405:329–339.

Klöckner, U., and G. Isenberg. 1985*b*. Calcium currents of cesium loaded isolated smooth muscle cells (urinary bladder of the guinea pig). *Pflügers Archiv.* 405:340–348.

Lee, K. S., E. Marban, and R. W. Tsien. 1985. Inactivation of calcium channel in mammalian heart cells: joint dependence on membrane potential and intracellular calcium. *Journal of Physiology.* 364:395–411.

Lee, K. S., and R. W. Tsien. 1982. Reversal of current through calcium channels in dialysed single heart cells. *Nature.* 297:498–501.

McCleskey, E. W., A. P. Fox, D. Feldman, and R. W. Tsien. 1986. Different types of calcium channels. *Journal of Experimental Biology.* 124:177–190.

McLaughlin, S. G. A., G. Szabo, and G. Eisenman. 1971. Divalent ions and the surface potential of charged phospholipid membrane. *Journal of General Physiology.* 58:667–687.

Mitra, R., and M. Morad. 1985. Ca^{2+} and Ca^{2+}-activated K^+ currents in mammalian gastric smooth muscle cells. *Science.* 229:269–272.

Momose, K., and Y. Gomi. 1980. Studies on isolated smooth muscle cells. IV. Dispersion procedures for acetylcholine-sensitive smooth muscle cells of guinea pig. *Japanese Journal of Smooth Muscle Research.* 16:29–36.

Nilius, B., P. Hess, J. B. Lansman, and R. W. Tsien. 1985. A novel type of cardiac calcium channel in ventricular cells. *Nature.* 316:443–446.

Obara, K. 1984. Isolation and contractile properties of single smooth muscle cells from guinea pig taenia caeci. *Japanese Journal of Physiology.* 34:41–54.

Obara, K., and T. Yamada. 1984. Some properties of chemically skinned single smooth muscle cells. *Japanese Journal of Physiology.* 34:1089–1104.

Ohya, Y., K. Terada, K. Kitamura, and H. Kuriyama. 1986. Membrane currents recorded from a fragment of rabbit intestinal smooth muscle cell. *American Journal of Physiology.* 251:C335–C346.

Reuter, H. 1973. Divalent cations as charge carriers in excitable membranes. *Progress in Biophysics and Molecular Biology.* 26:1–43.

Singer, J. J., and J. V. Walsh. 1980. Passive properties of the membrane of single freshly isolated smooth muscle cells. *American Journal of Physiology.* 239:C153–C161.

Sturek, M., and K. Hermsmeyer. 1986. Calcium and sodium channels in spontaneously contracting vascular muscle cells. *Science.* 233:475–477.

Tsien, R. W. 1983. Calcium channels in excitable cell membranes. *Annual Review of Physiology.* 45:341–358.

Walsh, J. V., and J. J. Singer. 1981. Voltage clamp of single freshly dissociated smooth muscle cells: current-voltage relationships for three currents. *Pflügers Archiv.* 390:207–210.

Walsh, J. V., and J. J. Singer. 1987. Identification and characterization of major ionic currents in isolated smooth muscle cells using the voltage-clamp technique. *Pflügers Archiv.* 408:83–97.

Yamamoto, Y., S. L. Hu, and C. Y. Kao. 1987*a*. Ionic currents in single cells from guinea pig taenia coli. *Biophysical Journal.* 51:200*a*. (Abstr.)

Yamamoto, Y., S. L. Hu, and C. Y. Kao. 1987*b*. Inactivation of the calcium current in single cells of the guinea pig taenia coli. *Federation Proceedings.* 46:507. (Abstr.)

Yamamoto, Y., S. L. Hu, and C. Y. Kao, 1988. Demonstration of multiple types of calcium channels in smooth muscle cells of the guinea pig taenia coli. *Biophysical Journal.* 53:594*a*. (Abstr.)

Yamamoto, Y., S. L. Hu, and C. Y. Kao. 1989. The outward current in single smooth muscle cells of the guinea pig taenia coli. *Journal of General Physiology.* 93:551–564.

Yoshino, M., and H. Yabu. 1985. Single Ca channel currents in mammalian visceral smooth muscle cells. *Pflügers Archiv.* 404:285–286.